scientific reports

Check for updates

OPEN

Glucose and NAADP trigger elementary intracellular β-cell Ca^{2+} signals

Paula Maria Heister[1,2]✉, Trevor Powell[1] & Antony Galione[1]✉

Pancreatic β-cells release insulin upon a rise in blood glucose. The precise mechanisms of stimulus-secretion coupling, and its failure in Diabetes Mellitus Type 2, remain to be elucidated. The consensus model, as well as a class of currently prescribed anti-diabetic drugs, are based around the observation that glucose-evoked ATP production in β-cells leads to closure of cell membrane ATP-gated potassium (K_{ATP}) channels, plasma membrane depolarisation, Ca^{2+} influx, and finally the exocytosis of insulin granules. However, it has been demonstrated by the inactivation of this pathway using genetic and pharmacological means that closure of the K_{ATP} channel alone may not be sufficient to explain all β-cell responses to glucose elevation. We have previously proposed that NAADP-evoked Ca^{2+} release is an important step in stimulus-secretion coupling in pancreatic β-cells. Here we show using total internal reflection fluorescence (TIRF) microscopy that glucose as well as the Ca^{2+} mobilising messenger nicotinic acid adenine dinucleotide phosphate (NAADP), known to operate in β-cells, lead to highly localised elementary intracellular Ca^{2+} signals. These were found to be obscured by measurements of global Ca^{2+} signals and the action of powerful SERCA-based sequestration mechanisms at the endoplasmic reticulum (ER). Building on our previous work demonstrating that NAADP-evoked Ca^{2+} release is an important step in stimulus-secretion coupling in pancreatic β-cells, we provide here the first demonstration of elementary Ca^{2+} signals in response to NAADP, whose occurrence was previously suspected. Optical quantal analysis of these events reveals a unitary event amplitude equivalent to that of known elementary Ca^{2+} signalling events, inositol trisphosphate (IP_3) receptor mediated blips, and ryanodine receptor mediated quarks. We propose that a mechanism based on these highly localised intracellular Ca^{2+} signalling events mediated by NAADP may initially operate in β-cells when they respond to elevations in blood glucose.

The idea that stimulus-secretion coupling involves mechanisms in addition to the K_{ATP} channel-mediated pathway[1,2] is not new[3,4]. Possible mechanisms include (1) an amplification of the K_{ATP} channel dependent pathway which remains functionally silent until the latter has depolarised the membrane[5],(2) an additional triggering pathway that converges with the K_{ATP} channel mediated pathway on membrane depolarisation, and (3) an independently functional pathway that may lead to insulin release in the absence of K_{ATP} channel involvement[6]. One potential trigger of stimulus-secretion coupling, which may be synergistic with, or independent of, K_{ATP} channel closure, is the local release of Ca^{2+} from intracellular stores[7]. Indeed, there has been some debate about the relative importance of extracellular Ca^{2+} influx versus release from intracellular stores during biphasic insulin secretion, with some proposing that for the first phase of insulin release, influx is dispensable[8]. In terms of subcellular localized Ca^{2+} signals, it was shown in the late 1970s using pyroantimonate precipitation that incubation of β-cells with high glucose led to a Ca^{2+} increase immediately beneath the cell membrane[9]. Levels of NAADP, a Ca^{2+} mobilizing intracellular messenger that releases Ca^{2+} from lysosomes and acidic organelles, have previously been shown to be elevated in pancreatic β-cells by increased extracellular concentrations of glucose during stimulus-secretion coupling[10,11]. Moreover, inhibition of NAADP signalling in β-cells suppresses Ca^{2+} spiking and membrane depolarization[7,10,12]. The possible role of small lysosomal Ca^{2+} stores in stimulus-secretion coupling[7] warranted the investigation of Ca^{2+} signalling in β-cells at high spatial and temporal resolution. Thus the present study sought to characterise sub-membrane Ca^{2+} transients observed in β-cells loaded with fluo-4 in response to glucose and the membrane permeable form of the lysosomal Ca^{2+} mobilizing messenger, NAADP (NAADP-AM)[13], using total internal reflection fluorescence (TIRF) microscopy[14]. Furthermore, we hypothesized that dissection of these Ca^{2+} transients under experimental conditions where globalized Ca^{2+} signals or ER-based

[1]Department of Pharmacology, Mansfield Road, Oxford OX1 3QT, UK. [2]Department of Pathology, Addenbrooke's Hospital, Hills Road, Cambridge CB2 0QQ, UK. ✉email: ph535@cam.ac.uk; antony.galione@pharm.ox.ac.uk

Ca^{2+} sequestration[15] were avoided, might reveal their substructure, akin to the sparks and puffs observed for IP_3 and ryanodine receptors, respectively[16,17,18].

A feature of Ca^{2+} signalling dynamics in pancreatic β-cells is their heterogeneity upon stimulation, with the recent proposal that some cells in the islet act as Ca^{2+} signalling hubs or pacemakers[19], whilst others follow through gap-junctional or paracrine signalling mechanisms. However, heterogeneity is also seen in isolated cells. Indeed, Ca^{2+} responses to glucose in β-cells have been described as having a typical triphasic shape often seen in parallel with, and assumed to be the result of, simultaneously measured changes in membrane potential, which have a similar pattern and are in synchrony with the cytosolic Ca^{2+} increase[15]: Phase 0 consists of a 'dip', or initial decrease, in cytosolic free Ca^{2+} resulting from increased sarco-/endoplasmic reticulum Ca^{2+} ATPase (SERCA) activity transporting Ca^{2+} into the endoplasmic reticulum (ER) in response to the rising ATP concentration following glucose metabolism. Phase 1 constitutes a transient rise in Ca^{2+} associated with L-type Ca^{2+} channel activation and Ca^{2+}-induced Ca^{2+} release (CICR) from intracellular stores. Phase 2 are Ca^{2+} oscillations superimposed on a steadily elevated plateau thought to be the result of Ca^{2+} influx through L-type channels. While this standardised model is useful; it has been demonstrated that β-cells display more complex responses to glucose and other stimuli such as GLP-1, insulin, and nutrients including amino acids[20,21]. A classification of primary human β-cell autocrine Ca^{2+} responses to insulin shows that β-cells display a variety of equally common but different Ca^{2+} signals and no clear 'standard' response[22].

Results

We report here sub-membrane Ca^{2+} transients evoked by 16.5 mM glucose in mouse primary pancreatic β-cells, measured using evanescent-wave TIRF microscopy. Recordings were made from 1,017 cells. Figure 1 shows the classification of typical responses of 239 cells from male WT mice of one genetic background, to avoid additional confounding factors. There was a clear heterogeneity of responses. While over 96% of cells exhibited a clear elevation of sub-membrane Ca^{2+} (calculated as $\Delta F/F_0$, where ΔF is the change in fluorescence intensity from pre-stimulation F_0), ~60% resembled the standardised triphasic profile, with the remaining responding cells described by 3 further classifications (cf. Fig. 1). These data are consistent with the notion that there are β-cells with different patterns of expression of Ca^{2+} channels, which may serve multiple functions within the islet[19]. Treatment of mouse primary pancreatic β-cells with extracellular NAADP-AM (10 μM) resulted in similar Ca^{2+} responses to those observed with glucose described above. Ca^{2+} oscillations could be resolved that culminated in a raised plateau of elevated $[Ca^{2+}]_i$ in 89% of cells (see, for example, a 'type 4' response elicited by NAADP-AM in Fig. S1). Response type distributions for stimulation with NAADP-AM were as follows: Type 1, 27%; Type 2, 0%; Type 3, 5%; Type 4, 59%, no response, 9%, n = 53.

If Ca^{2+} release from sub-membrane stores triggered the global Ca^{2+} response, an increase in Ca^{2+} could be expected to occur first in the vicinity of the cell membrane, the location of the cell's secretory vesicles which form part of the acidic organelle continuum in the β-cell[23], before recruiting a global Ca^{2+} response[24]. Lysotracker was utilised to confirm the presence of acidic stores within the TIRF plane (see Fig. S2). In parallel recordings using TIRF and standard epifluorescence (to monitor global Ca^{2+}), however, the two transients were largely superimposable (see supplementary data, Fig. S3). Thus if there were sub-membrane Ca^{2+} release events preceding the global Ca^{2+} response, they were either very rapid and too small to be detected by the current protocol, masked by concomitant larger L-type Ca^{2+} channel-mediated influx, or obscured by increased SERCA pump activity following enhanced glucose metabolism to ATP.

In order to minimise these possible confounding factors, cells were pre-incubated in recording medium containing 1.7 mM Ca^{2+}, 3 mM glucose, and 1 μM of the irreversible SERCA inhibitor, thapsigargin. Immediately before recording, the extracellular fluid was exchanged for Ca^{2+}-free medium, containing thapsigargin and either 100 μM or 5 mM EGTA. The removal of Ca^{2+} immediately before recording prevented non-ER stores, which may rely on Ca^{2+} influx and ER Ca^{2+} transfer for filling[25,26], from run-down during the incubation period. Cells were then challenged with either 100 nM NAADP-AM or 16.5 mM extracellular glucose. Over the ~10 min period following either challenge, cells showed clear very brief sub-membrane Ca^{2+} transients with maximum amplitudes > $2\Delta F/F_0$. These show comparable kinetics to those of Ca^{2+} puffs evoked by IP_3[27]. The movie (supplementary information, Movie 1) illustrates recordings of these events, and examples are shown in Fig. 2a–i. Their localised nature is illustrated in the maximum $\Delta F/F_0$ trace (Fig. 2m) and the 3D fluorescence intensity plots shown in Fig. 2 j–l. Similar localized Ca^{2+} signals were observed in extracellular solutions containing 100 μM and 5 mM EGTA (cf Fig. S4), strongly suggesting that Ca^{2+} release from intracellular stores but not Ca^{2+} influx are involved in the generation of these elementary Ca^{2+} events. These local transients were also recorded at a higher acquisition rate (46 Hz) (Fig. S5, Movie 2), giving additional resolution of the events captured at our standard experimental recording rates of 3.3 Hz.

To resolve these individual events in more detail, a spark detection algorithm was used (see Methods) which also removed the underlying 'ramp' in cell Ca^{2+} that can be seen in Fig. 2m. There is an increasing frequency of events following application of 100 nM NAADP-AM or 16.5 mM glucose to a maximum; followed by a gradual decline (Figs. 3a, b, S6). This is in accordance with the self-limiting nature of these types of signals when stores cannot be replenished during sustained stimulation[28] or desensitization to signals such as NAADP[22,29]. To quantify the changes in frequency, the mean percentage of frames showing at least one spike (defined as an event 2 standard deviations above mean baseline $\Delta F/F_0$) was determined for the baseline (last 80–100 frames before stimulus) and after the addition of raised glucose or NAADP-AM. As illustrated in Fig. 3e, f, both 100 nM NAADP-AM and 16.5 mM glucose evoked an approximately ten-fold increase in spike frequency.

Having unmasked discrete Ca^{2+} signals in response to a high concentration of glucose (16.5 mM) after thapsigargin pre-incubation, this raises the question of whether similar responses could be evoked by a smaller increase in extracellular glucose without the use of thapsigargin. We examined whether a doubling of glucose from 3 to

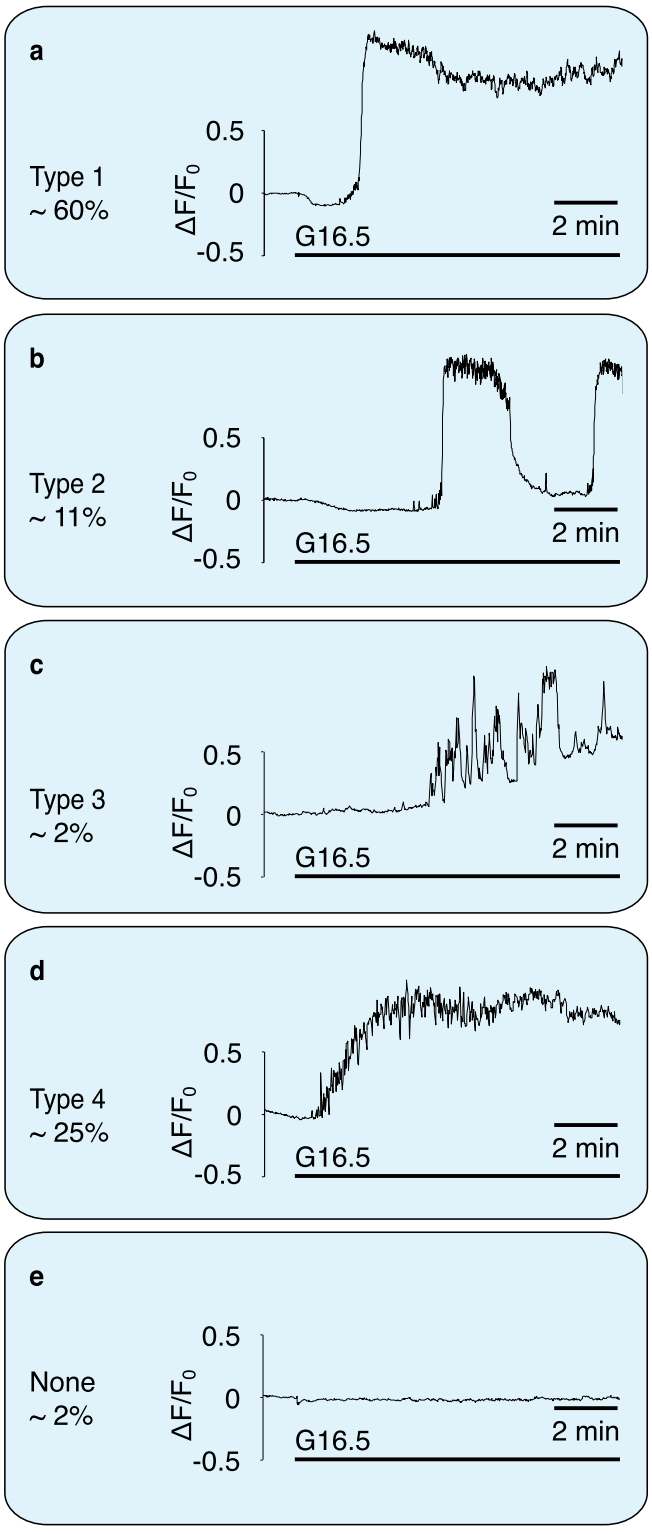

Figure 1. Classification of β-cell sub-membrane Ca^{2+} responses to elevation in glucose as recorded with TIRF. Responses to 16.5 mM glucose at 37° C in mouse primary pancreatic β-cells. n = 239. Responses from 1,017 cells were analysed overall. Percentages are of 239 control cells of male WT mice of one genetic background to exclude potential genetic- or sex differences in response type distribution. Approximately 96% showed a prominent global calcium response. In 116 cells, 16.5 mM glucose evoked a mean peak height of 2.4 ± 0.01 $\Delta F/F_0$. (**a**) The most common response (type 1, ca. 60% of responses) resembles the standardized triphasic response. (**b**) The slow Ca^{2+} oscillations classified as type 2 often occurred at periods of ca. 5 min. (**c**) Response type 3 consists of numbers of large transients superimposed on a slow increase in Ca^{2+}. These responses were rare (ca. 2%). (**d**) Type 4 responses (ca. 25%) resemble the triphasic response, but with a less steep Ca^{2+} rise. (**e**) A very small number of cells did not respond to glucose (ca. 2%).

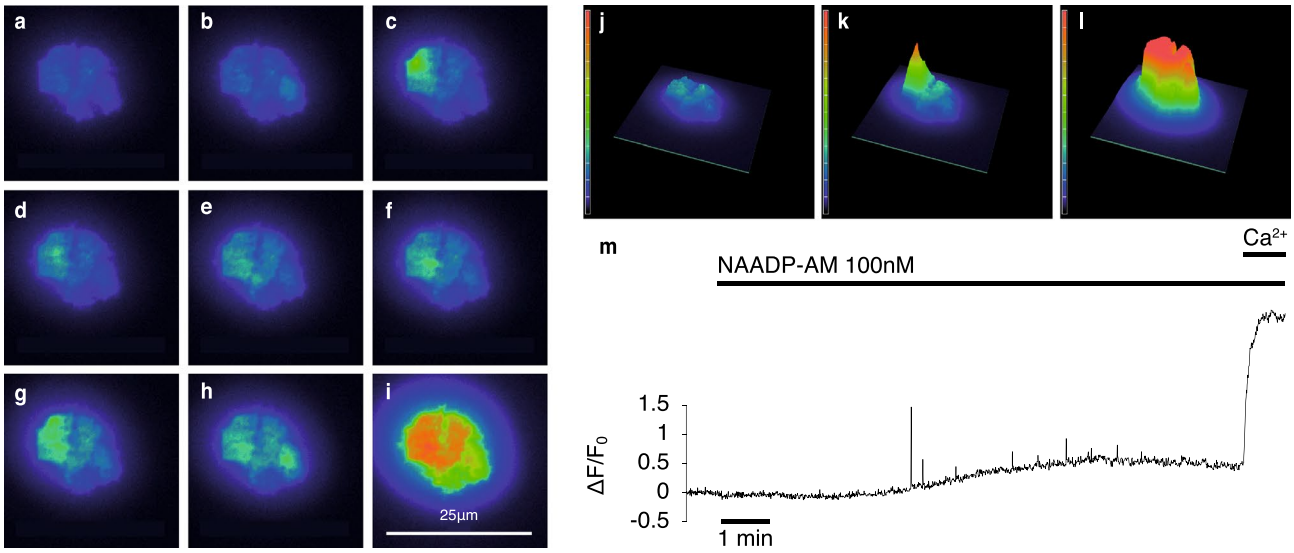

Figure 2. Localised and global Ca^{2+} responses. Responses of a β-cell cluster (3 cells) after NAADP-AM addition as observed using TIRF microscopy in the presence of 5 mM EGTA. (**a**) Baseline fluorescence. (**b**–**h**) Localized Ca^{2+} release events (for illustrative purposes, larger events were selected). (**i**) Global Ca^{2+} influx. (**j**–**l**) Intensity profiles of a β-cell cluster, (**j**) at baseline, (**k**) in the presence of an elementary event after addition of NAADP-AM, (**l**) during global Ca^{2+} influx. Images are pseudocoloured with warmer colours representing higher levels of fluorescence. (**m**) Representative trace of a β-cell showing spiking Ca^{2+} events triggered by NAADP-AM. Maximum intensity change normalised to baseline is plotted against time. Extracellular Ca^{2+} was re-admitted at the end of the experiment; leading to a global Ca^{2+} response.

6 mM (a stimulatory concentration within the physiological range) without thapsigargin pre-incubation, would still allow us to detect visible Ca^{2+} events with TIRF. We reasoned that at lower concentrations of glucose, less ATP would be produced, resulting in lower SERCA activity, which would otherwise obscure detection of local Ca^{2+} events. As shown in Fig. 3c, the effects of stimulation with low glucose in the absence of thapsigargin resemble those of stimulation with high glucose in the presence of thapsigargin. The percentage of frames containing spikes is significantly higher after raising extracellular glucose to 6 mM (15%) than at baseline (4%; Fig. 3g). Using epifluorescence microscopy, no local Ca^{2+} release events could be detected (Fig. 3d).

To analyse the nature of the elementary Ca^{2+} events, optical quantal analysis was carried out on images like those shown in Fig. 4d, e (Fig. 4a, b show the same cells under brightfield microscopy and TIRF, respectively). Plotting the frame-maxima across all cells stimulated with NAADP-AM results in the frequency distribution depicted in Fig. 4f. Modes are visible in the 'tail' of this decaying function which occur at a period of around 0.05 $\Delta F/F_0$ (see figure inset). This order of magnitude is comparable to optically-assessed Ca^{2+} blips through IP_3 receptors (0.1 $\Delta F/F_0$[27]) and the smallest imaged IP_3-evoked Ca^{2+} signals in pancreatic acinar cells (< 0.1$\Delta F/F_0$[30]). To demonstrate the quantal nature of the Ca^{2+} responses at the level of the individual cell, responses from a representative cell cluster are shown in Fig. 4g. Specific regional areas of interest (ROIs) within the cell were chosen by hand on the basis of their containing at least one Ca^{2+} signalling event. These ROIs were then analysed for their mean amplitudes after subtraction of baseline fluorescence. Events were included if they lay above baseline mean + 2 SDs) of that particular cell. The frequency distribution displays modal behaviour as illustrated by the poly-Gaussian function fitted to it, and the putative unitary event amplitude for this cell cluster is 0.03 $\Delta F/F_0$.

Discussion

The above experiments demonstrate that β-cells show great variability in their Ca^{2+} responses and a high level of spontaneous activity; supporting the notion of a β-cell's 'Ca^{2+} fingerprint'[31]. As β-cells are frequently examined in artificially amplified resting and active states during experiments[6,32], we have shown here that stimulation with the high glucose concentrations often employed, leading to high SERCA activity[33], obscures more subtle Ca^{2+} changes taking place within the cell. It is probable that multiple stores and channels play a part in this process[32,34]. The fact that the events occur after pre-incubation with thapsigargin, ruling out the ER as a source, are most striking when triggered with NAADP-AM which targets acidic stores, and are localised just beneath the membrane (the primary location of insulin granules, a subset of the acidic organelles in the β-cell[35]), is a strong suggestion that the source of these events are acidic Ca^{2+} storage organelles. However, further pharmacological studies are required to fully delineate the origin of these signals.

With the discovery of two-pore channels (TPCs) as the putative target for NAADP[36,37], and the present discovery of elementary Ca^{2+} release events in response to NAADP; it is likely that NAADP-evoked Ca^{2+} signals from acidic stores are built from elementary events via activation of TPCs. It was suggested in 1996 that NAADP-mediated Ca^{2+} release was quantal on the basis of its graded release from sea urchin homogenate[38] and in intact sea urchin eggs localized Ca^{2+} responses ascribed to the osmotic lysis of acidic stores by GPN[39]; 25 years on, we may have evidence in a mammalian cell type that a similar principle operates. Thus with the existing sets of

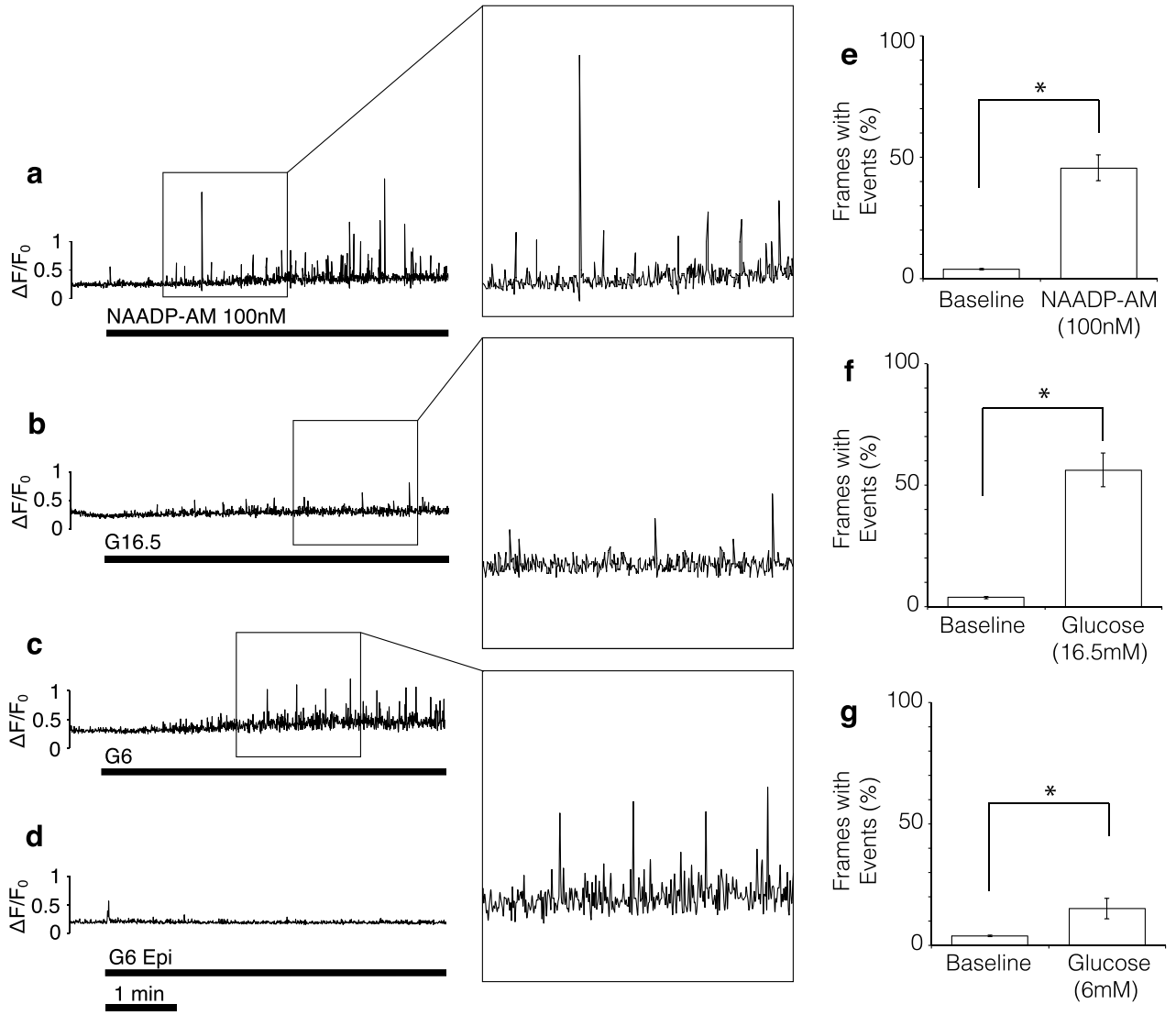

Figure 3. Quantification of calcium release events in response to glucose and NAADP-AM in low EGTA (100 µM). (**a**–**c**) Representative TIRF traces of β-cells stimulated with: (**a**) 100 nM NAADP-AM after preincubation with thapsigargin, (**b**) 16.5 mM glucose after preincubation with thapsigargin, (**c**) 6 mM glucose without thapsigargin preincubation. (**d**) Epifluorescence recording (all other parameters equal) using 6 mM glucose without thapsigargin preincubation. Maximum intensity change of subsequent frames after normalising to baseline plotted against time. Insets show magnified events for each of the three experimental stimuli, chosen to illustrate the variation in event size. (**e**–**g**) Percentage of frames showing elementary events (defined as events of an amplitude more than 2 standard deviations above baseline mean) before (baseline) and after stimulus addition. (**e**) NAADP-AM; n = 20 (8 experiments, 4 Animals), $t(19) = 7.90$, $p < 0.01$, 90% response rate. (**f**) 16.5 mM glucose; n = 14 (6 experiments, 4 Animals), $t(13) = 7.44$, $p < 0.01$, 100% response rate. (**g**) 6 mM glucose; n = 18 (6 experiments, 6 Animals), $t(17) = 2.61$, $p < 0.01$, 50% response rate. * denotes significance; paired samples, one-tailed t-tests.

elementary Ca^{2+} signals: IP_3, the IP_3R, and blips; cADPR, the RyR, and quarks, respectively, elementary Ca^{2+} release events appear to be a governing principle of intracellular Ca^{2+} signalling, regardless of channels involved or Ca^{2+} storage organelle.

In addition to demonstrating elementary Ca^{2+} signals in response to NAADP for the first time, the present study also suggests a potential role for these events in stimulus-secretion coupling in β-cells. NAADP has been shown to elicit Ca^{2+} signals and insulin release in mouse pancreatic β-cells[7,22,10,11]. Whilst there is argument over the identity of NAADP's target in the β-cells[7,40,41], mutations in the two-pore channel gene (TPCN2), the potential principal target for NAADP, have been implied in the inheritance of diabetes type 2 in humans[42]. Localized Ca^{2+} signals from acidic stores have been proposed to cause depolarisation by activating calcium-dependent cation channels in the plasma membrane as we have previously observed[7,43], such as TRPM4[7] and TRPM5[44,46,47]. NAADP applied through a patch-pipette evoked small oscillatory cation currents which were preceded by small Ca^{2+} transients[7] which were abolished in cells from *Tpcn2*$^{-/-}$ mice. Importantly, elevating glucose concentrations

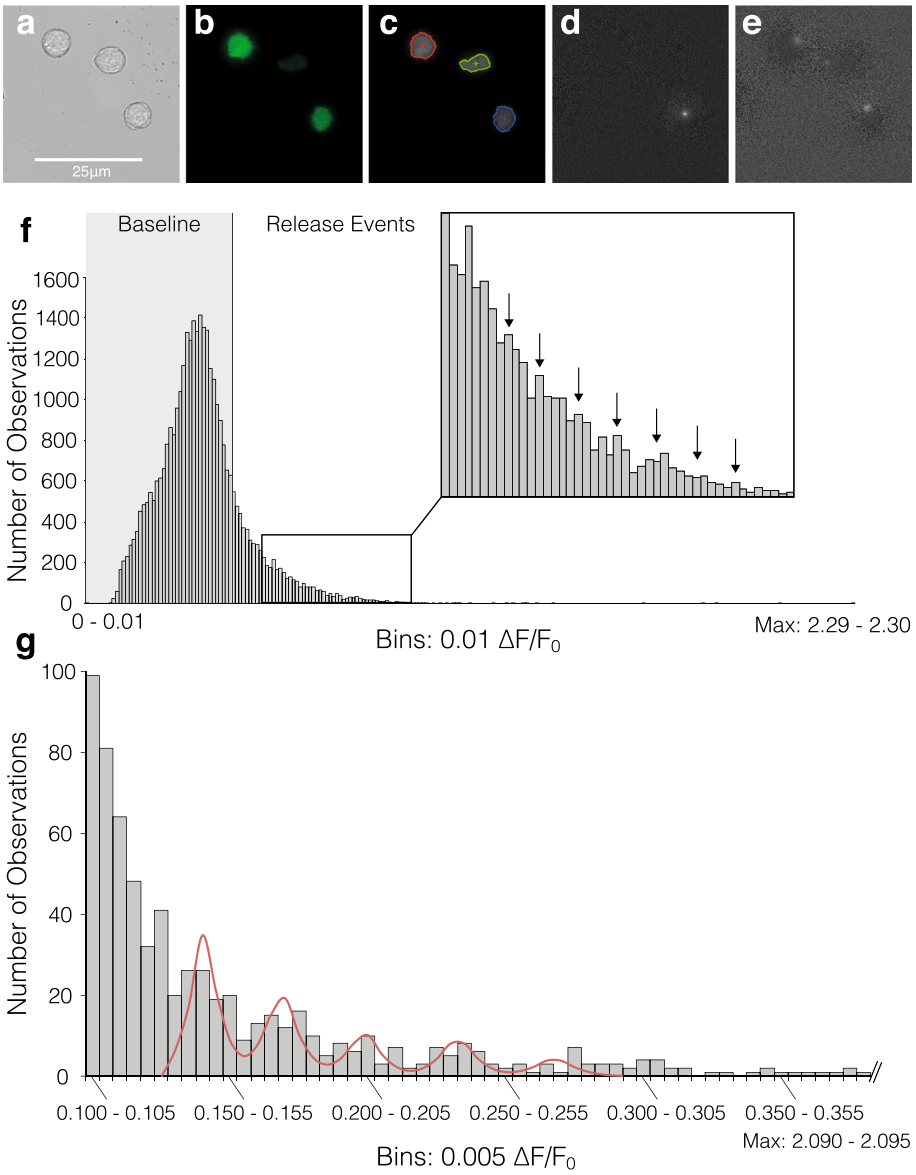

Figure 4. Quantal analysis of elementary events. (**a**–**e**) Illustration of spark analysis, including examples of elementary release events in response to 16.5 mM glucose detected by normalisation, frame by frame and background subtraction in 3 individual β-cells: (**a**) Original brightfield, (**b**) TIRF, (**c**) Boundaries used in detection analysis, (**d**–**e**) Individual events isolated by analysis. Note that images of glucose-induced events were chosen for illustration of the analysis mechanism; quantal analysis was carried out exclusively on NAADP-AM stimulated cells. (**f**) Frequency histogram of maximum intensity change after NAADP-AM Stimulation (n = 20), the vertical line at 0.44 $\Delta F/F_0$ denotes 2 standard deviations above baseline mean. (**g**) Frequency histogram of mean event amplitudes across areas of interest (n = 51) within a single cell cluster stimulated with NAADP-AM in the presence of 5 mM EGTA. The five peaks of the putative modal distribution in the data were selected as means for individual Gaussian distributions; and 3–4 bins to their left and right used to calculate the respective distribution's standard deviation. The resultant means and standard deviations were used to fit a quintuple Poly-Gaussian function (Sum of five Gaussian functions with Means, SDs: 0.143, 0.007; 0.171, 0.008; 0.201, 0.0089; 0.235, 0.0092; 0.270, 0.0103, respectively) to the data. Histogram was cropped for better resolution-values below event cutoff (2 standard deviations above baseline mean: 0.1 $\Delta F/F_0$) are not included and actual maximum intensity bin is 2.09–2.095.

evoked similar cation currents, which along with those evoked by NAADP were inhibited by the NAADP antagonist, Ned-19[7]. We have now imaged these localized Ca^{2+} events with our TIRF methodologies in the current study. However, local Ca^{2+} release from acidic stores is also known to trigger CICR in many cells, likely involving membrane contact sites with the ER[48]. In yet other cell types, NAADP was shown to induce localized Ca^{2+} release from secretory granules to initiate their own exocytosis[49]. In pancreatic β-cells, ER Ca^{2+} leak and subsequent uptake into mitochondria via the mitochondrial Ca^{2+} uniporter (MCU) complex have been proposed to prime

ATP synthesis[50]. Since it has been suggested that TPCs can be blocked by ATP[51], there may be a complex interplay between Ca^{2+} release from acidic stores and the dynamics of ATP concentrations at the subcellular level.

Thus we propose that during stimulus-secretion coupling in β-cells K_{ATP} channel closure induced by a rise in local ATP levels increases membrane resistance allowing small cation currents, activated by localized Ca^{2+} signals (a summation of elementary Ca^{2+} events from intracellular stores and CICR) to initiate depolarization of the plasma membrane. This in turn results in the opening of L-type Ca^{2+} channels whose mediation of larger globalized Ca^{2+} signals triggers insulin granule exocytosis. This model differs from, but contains elements of, each of the three models of a K_{ATP} channel independent pathway previously discussed. The present investigation suggests that glucose initially generates localized Ca^{2+} signalling events based on Ca^{2+} release from non-ER, likely acidic, stores prior to the influx of Ca^{2+} through VGCCs. We propose that some of the elementary trigger events involved are likely to be mediated by NAADP as we have previously suggested[7,24,45].

Methods

Primary β-cell culture. Mouse pancreatic islets from 10–14 week-old WT male mice (of a mixed C57BL/6;129P2 background obtained from the European Mouse Mutant Archive, EMMA) were isolated as described previously[52]. Islets were dispersed into single cells or cell clusters and plated onto poly-L-lysine coated glass coverslips (Menzel) and incubated in cellstar dishes (Greiner) at 37 °C for 4–7 h before adding cell culture medium (RPMI 1640, -glucose + glutamine, Gibco), supplemented with penstrep (10,000 U/ml penicillin/10,000 µg/ml streptomycin, Gibco) and 10% fetal bovine serum (FBS, Gibco) containing 10 mM glucose and incubated for a further 15–17 h before first use. Cells were loaded with 500 nM fluo 4-AM (Invitrogen) for 1 h in the dark, before being washed with imaging buffer (NaCl 130 mM, KCl 5.2 mM, $MgCl_2$ 1 mM, HEPES 10 mM, $CaCl_2$ 1.7 mM; pH: 7.4, 280–340 mOsm/kg) containing 3 mM glucose and left in this for 10 min before start of recording. Experiments were conducted exclusively at 37 °C, and with a baseline glucose concentration of 3 mM, simulating physiological conditions. Experiments to demonstrate localised elementary events were conducted on both single cells and small clusters; at an estimated ratio of 50% cells, 50% clusters. Clusters lend themselves to TIRF experiments, as they provide a large area positioned in the same focal-plane. Dispersed cells are usually at marginally different focal planes due to the inherent curvature of the glass coverslip. In studies using Ca^{2+}-free medium, extracellular Ca^{2+} was re-admitted at the end of the experiment to visualise a global response as a verification of the cell's viability. In experiments to visualise acidic stores, cells were preincubated for 10–30 min with LysoTracker Red (Invitrogen) at 200 nM. NAADP-AM was synthesised as previously described[13]. Batches varied in potency due to different efficiencies of synthesis and storage degradation as determined by HPLC analysis.

Imaging. Cells were excited with an Argon-Ion laser (Andor DU-897, 40 mW; Melles Griot) at 488 nm, and images were obtained using a Nikon Evanescent Wave Imaging System; an Inverted Total Internal Reflection Microscope (Nikon Eclipse Ti) equipped with 60 × and 100 × CFI Apochromat TIRF Series oil-immersion lenses. These lenses have a numerical aperture of 1.49, which allowed for a maximal incident angle of 76.87° calculated by $\alpha \geq \sin^{-1}(n_2/n_1)$, $n_1 > n_2$, where n_1 is the refractive index of the cover glass (1.53), and n_2 the numerical aperture of the lens (1.49). The exact angle for experimentation was determined using a Bertrand lens and the beam adjusted. This allowed for an evanescent wave illuminating the specimen to a depth of around 100 nm. All parameters were controlled using NIS Elements AR 4.0 (Nikon). Images were acquired at a rate of 3.3 Hz for single channel recordings (i.e. only TIRF or Epifluorescence) and at a pre-programmed rate for dual channel recordings (Frame Rate Epi: 1 Hz. Frame Rate TIRF: 3.3 Hz). Data in Fig. S5 and Movie 2 were acquired using NIS Elements RAM capture mode (acquisition rate ~ 46 Hz). A CCD camera (Andor iXon +) was used to capture emitted fluorescence at 515–555 nm (Binning: 1 × 1, Exposure: 300 ms, Multiplier: 89, Readout Speed: 10 Hz, Conversion Gain: 1x, Dimensions: 512 × 512, 160 nm/pixel).

Analysis. For quantal analysis, fluorescence change across each whole cell (selected as an area of interest, ROI, see Fig. 4c) was analysed by first normalising each image (time frame) pixel by pixel with respect to the average fluorescence across the last 80–100 frames before cell stimulation with glucose or NAADP-AM (cells stimulated using glucose were not used for quantal analysis, as it is an unspecific stimulus and may trigger events via multiple pathways). To eliminate the moving baseline (ramp), a frame by frame subtraction function was used. Of these normalised, baseline-controlled images, the maximum intensity within each cell was measured. A similar algorithm has been used for 2D images previously[53], and while this paper was in preparation, an automated system applying a sophisticated version of it was released[54]. From the measured maximum intensities for each cell over time, frequency histograms were compiled to depict the quantal nature of the events, where events more than 2 standard deviations above the baseline mean were considered genuine. This is a standard estimate of minimum spark amplitude[30]. All analysis was conducted in NIS Elements AR 4.0 (Nikon) and MS Excel 14 (Microsoft). Figures were prepared in Illustrator CS6 (Adobe). Ca^{2+} traces are of fluorescence change relative to baseline mean fluorescence ($\Delta F/F_0$). Baseline mean fluorescence (F_0) was calculated from the fluorescence of the last 80–100 frames before stimulation. Traces are representative, as indicated in figure legends. Ca^{2+} fluorescence images are pseudo-coloured so that changes in colour reflect changes in fluorescence. Warmer colours represent higher levels of fluorescence. Statistical analysis was conducted in MS Excel 14 and SPSS 19 (IBM). Student's t-tests (paired or unpaired, one- or two-tailed, as applicable) were used to determine the statistical significance of observed effects ($p < 0.05$, $p < 0.01$, as stated). Charts illustrating statistical differences between groups depict mean ± standard error of the mean (SEM) unless stated otherwise. Videos for supplementary information were prepared from Nikon .nd2 files and rendered using Premiere Pro CS6 (Adobe).

Animal experiments. The procedures to prepare primary β-cell cultures from mice were conducted in line with the UK Animals (Scientific Procedures) Act 1986, using exclusively Schedule 1 methods, and approved by the University of Oxford's Local Ethical Review Committee.

Received: 17 November 2020; Accepted: 15 April 2021
Published online: 21 May 2021

References

1. Ashcroft, F. M., Harrison, D. E. & Ashcroft, S. J. Glucose induces closure of single potassium channels in isolated rat pancreatic beta-cells. *Nature* **312**, 446–448 (1984).
2. Cook, D. L. & Hales, C. N. Intracellular ATP directly blocks K^+ channels in pancreatic β-cells. *Nature* **311**, 271–273 (1984).
3. Henquin, J. C. A minimum of fuel is necessary for tolbutamide to mimic the effects of glucose on electrical activity in pancreatic beta-cells. *Endocrinology* **139**, 993–998 (1998).
4. Seghers, V., Nakazaki, M., DeMayo, F., Aguilar-Bryan, L. & Bryan, J. Sur1 knockout mice. A model for K_{ATP} channel-independent regulation of insulin secretion. *J. Biol. Chem*. **275**, 9270–9277 (2000).
5. Henquin, J. C. Triggering and amplifying pathways of regulation of insulin secretion by glucose. *Diabetes* **49**, 1751–1760 (2000).
6. Islam, M. S. Calcium signaling in the islets. *Adv. Exp. Med. Biol.* **654**, 235–259 (2010).
7. Arredouani, A. *et al.* Nicotinic acid adenine dinucleotide phosphate (NAADP) and endolysosomal two-pore channels modulate membrane excitability and stimulus-secretion coupling in mouse pancreatic beta cells. *J. Biol. Chem*. **290**, 21376–21392 (2015).
8. Wollheim, C. B., Kikuchi, M., Renold, A. E. & Sharp, G. W. The roles of intracellular and extracellular Ca^{++} in glucose-stimulated biphasic insulin release by rat islets. *J. Clin. Invest*. **62**, 451–458 (1978).
9. Wollheim, C. B. & Sharp, G. W. Regulation of insulin release by calcium. *Physiol. Rev.* **61**, 914–973 (1981).
10. Masgrau, R., Churchill, G. C., Morgan, A. J., Ashcroft, S. J. & Galione, A. NAADP: a new second messenger for glucose-induced Ca^{2+} responses in clonal pancreatic beta cells. *Curr. Biol*. **13**, 247–251 (2003).
11. Park, K. H. *et al.* Autocrine/paracrine function of nicotinic acid adenine dinucleotide phosphate (NAADP) for glucose homeostasis in pancreatic beta-cells and adipocytes. *J. Biol. Chem*. **288**, 35548–35558 (2013).
12. Naylor, E. *et al.* Identification of a chemical probe for NAADP by virtual screening. *Nat Chem Biol* **5**, 220-226 (2009).
13. Parkesh, R. *et al.* Cell-permeant NAADP: a novel chemical tool enabling the study of Ca^{2+} signalling in intact cells. *Cell Calcium* **43**, 531–538 (2008).
14. Axelrod, D. Cell-substrate contacts illuminated by total internal reflection fluorescence. *J. Cell Biol*. **89**, 141–145 (1981).
15. Worley, J. F. 3rd. *et al.* Endoplasmic reticulum calcium store regulates membrane potential in mouse islet beta-cells. *J Biol Chem* **269**, 14359–14362 (1994).
16. Cheng, H., Lederer, W. J. & Cannell, M. B. Calcium sparks: elementary events underlying excitation-contraction coupling in heart muscle. *Science* **262**, 740–744 (1993).
17. Parker, I., Choi, J. & Yao, Y. Elementary events of $InsP_3$-induced Ca^{2+} liberation in Xenopus oocytes: hot spots, puffs and blips. *Cell Calcium* **20**, 105–121 (1996).
18. Parker, I. & Ivorra, I. Localized all-or-none calcium liberation by inositol trisphosphate. *Science* **250**, 977–979 (1990).
19. Rutter, G. A. *et al.* Local and regional control of calcium dynamics in the pancreatic islet. *Diabetes Obes Metab* **19**(Suppl 1), 30–41 (2017).
20. Gustavsson, N., Larsson-Nyren, G. & Lindstrom, P. Cell specificity of the cytoplasmic Ca^{2+} response to tolbutamide is impaired in beta-cells from hyperglycemic mice. *J Endocrinol* **190**, 461–470 (2006).
21. Herchuelz, A., Pochet, R., Pastiels, C. & Van Praet, A. Heterogeneous changes in $[Ca^{2+}]_i$ induced by glucose, tolbutamide and K^+ in single rat pancreatic β cells. *Cell Calcium* **12**, 577–586 (1991).
22. Johnson, J.D. & Misler, S. Nicotinic acid-adenine dinucleotide phosphate-sensitive calcium stores initiate insulin signaling in human beta cells. *Proc. Natl. Acad. Sci. USA*. **99**, 14566–14571 (2002).
23. Orci, L. *et al.* Conversion of proinsulin to insulin occurs coordinately with acidification of maturing secretory vesicles. *J Cell Biol* **103**, 2273–2281 (1986).
24. Arredouani, A. *et al.* An emerging role for NAADP-mediated Ca^{2+} signaling in the pancreatic beta-cell. *Islets* **2**, 323–330 (2010).
25. Morgan, A. J. *et al.* Bidirectional Ca^{2+} signaling occurs between the endoplasmic reticulum and acidic organelles. *J Cell Biol* **200**, 789–805 (2013).
26. Xu, H. & Ren, D. Lysosomal physiology. *Annu Rev Physiol* **77**, 57–80 (2015).
27. Smith, I. F. & Parker, I. Imaging the quantal substructure of single IP_3R channel activity during Ca^{2+} puffs in intact mammalian cells. *Proc Natl Acad Sci USA* **106**, 6404–6409 (2009).
28. Cheng, H. & Lederer, W. J. Calcium sparks. *Physiol Rev* **88**, 1491–1545 (2008).
29. Cancela, J. M., Churchill, G. C. & Galione, A. Coordination of agonist-induced Ca^{2+}-signalling patterns by NAADP in pancreatic acinar cells. *Nature* **398**, 74–76 (1999).
30. Fogarty, K. E., Kidd, J. F., Tuft, R. A. & Thorn, P. A bimodal pattern of $InsP_3$ -evoked elementary Ca^{2+} signals in pancreatic acinar cells. *Biophys J* **78**, 2298–2306 (2000).
31. Prentki, M. *et al.* Cell-specific patterns of oscillating free Ca^{2+} in carbamylcholine-stimulated insulinoma cells. *J Biol Chem* **263**, 11044–11047 (1988).
32. Islam, M. S. Stimulus-secretion coupling in beta-cells: from basic to bedside. *Adv Exp Med Biol* **1131**, 943–963 (2020).
33. Roe, M. W., Mertz, R. J., Lancaster, M. E., Worley, J. F. 3rd. & Dukes, I. D. Thapsigargin inhibits the glucose-induced decrease of intracellular Ca^{2+} in mouse islets of Langerhans. *Am J Physiol* **266**, E852-862 (1994).
34. Galione, A. NAADP receptors. *Cold Spring Harb Perspect Biol* **11**, a035071 (2019).
35. Orci, L. The insulin factory: a tour of the plant surroundings and a visit to the assembly line. The Minkowski lecture 1973 revisited. *Diabetologia* **28**, 528–546 (1985).
36. Calcraft, P. J. *et al.* NAADP mobilizes calcium from acidic organelles through two-pore channels. *Nature* **459**, 596–600 (2009).
37. Ruas, M. *et al.* Expression of Ca^{2+}-permeable two-pore channels rescues NAADP signalling in TPC-deficient cells. *Embo J* **34**, 1743–1758 (2015).
38. Genazzani, A. A., Empson, R. M. & Galione, A. Unique inactivation properties of NAADP-sensitive Ca^{2+} release. *J Biol Chem* **271**, 11599–11602 (1996).
39. Churchill, G. C. *et al.* NAADP mobilizes Ca^{2+} from reserve granules, lysosome-related organelles, in sea urchin eggs. *Cell* **111**, 703–708 (2002).
40. Cane, M. C., Parrington, J., Rorsman, P., Galione, A. & Rutter, G. A. The two pore channel TPC2 is dispensable in pancreatic beta-cells for normal Ca^{2+} dynamics and insulin secretion. *Cell Calcium* **59**, 32–40 (2016).

41. Guse, A. H. & Diercks, B. P. Integration of nicotinic acid adenine dinucleotide phosphate (NAADP)-dependent calcium signalling. *J Physiol* **596**, 2735–2743 (2018).
42. Fan, Y. *et al.* Genetic variants of TPCN2 associated with type 2 diabetes risk in the Chinese population. *PLoS ONE* **11**, e0149614 (2016).
43. Foster, W.J. *et al.* Hippocampal mGluR1-dependent long-term potentiation requires NAADP-mediated acidic store Ca^{2+} signaling. *Sci Signal* **11**, eaat9093 *(2018)*.
44. Brixel, L. R. *et al.* TRPM5 regulates glucose-stimulated insulin secretion. *Pflugers Arch* **460**, 69–76 (2010).
45. Davis, L. C., Morgan, A. J. & Galione, A. NAADP-regulated two-pore channels drive phagocytosis through endo-lysosomal Ca^{2+} nanodomains, calcineurin and dynamin. *Embo J.* **39**, e104058 (2020).
46. Colsoul, B. *et al.* Loss of high-frequency glucose-induced Ca^{2+} oscillations in pancreatic islets correlates with impaired glucose tolerance in $Trpm5^{-/-}$ mice. *Proc Natl Acad Sci USA* **107**, 5208–5213 (2010).
47. Enklaar, T., Brixel, L. R., Zabel, B. U. & Prawitt, D. Adding efficiency: the role of the CAN ion channels TRPM4 and TRPM5 in pancreatic islets. *Islets* **2**, 337–338 (2010).
48. Patel, S. & Brailoiu, E. Triggering of Ca^{2+} signals by NAADP-gated two-pore channels: a role for membrane contact sites? *Biochem Soc Trans* **40**, 153–157 (2012).
49. Davis, L. C. *et al.* NAADP activates two-pore channels on T cell cytolytic granules to stimulate exocytosis and killing. *Curr Biol* **22**, 2331–2337 (2012).
50. Klec, C. *et al.* Presenilin-1 established ER-Ca^{2+} leak: a follow up on its importance for the initial insulin secretion in pancreatic islets and beta-cells upon elevated glucose. *Cell Physiol Biochem* **53**, 573–586 (2019).
51. Cang, C. *et al.* mTOR regulates lysosomal ATP-sensitive two-pore Na^{+} channels to adapt to metabolic state. *Cell* **152**, 778–790 (2013).
52. Ravier, M. A. & Rutter, G. A. Isolation and culture of mouse pancreatic islets for ex vivo imaging studies with trappable or recombinant fluorescent probes. *Methods Mol Biol* **633**, 171–184 (2010).
53. Banyasz, T., Chen-Izu, Y., Balke, C. W. & Izu, L. T. A new approach to the detection and statistical classification of Ca^{2+} sparks. *Biophys J* **92**, 4458–4465 (2007).
54. Ellefsen, K. L., Settle, B., Parker, I. & Smith, I. F. An algorithm for automated detection, localization and measurement of local calcium signals from camera-based imaging. *Cell Calcium* **56**, 147–156 (2014).

Acknowledgements

This work was funded by a Medical Research Council Programme Grant (Grant Ref: G0901521) and Wellcome Trust Senior Investigatorship (Ref: 102828/Z/13/Z) to AG. PMH was supported by a Department of Pharmacology, University of Oxford DPhil Studentship. We would like to thank Professor Patrik Rorsman for support with experiments and Dr Anthony Morgan for comments on the manuscript.

Author contributions

A.G., T.P. and P.M.H. designed the experiments. P.M.H. conducted the experiments. A.G. and T.P. supervised the project. P.M.H., T.P. and A.G. prepared the manuscript. All authors reviewed the results and approved the final version of the manuscript.

Competing interests

The authors declare no competing interests.

Additional information

Supplementary Information The online version contains supplementary material available at https://doi.org/10.1038/s41598-021-88906-0.

Correspondence and requests for materials should be addressed to P.M.H. or A.G.

Reprints and permissions information is available at www.nature.com/reprints.

Publisher's note Springer Nature remains neutral with regard to jurisdictional claims in published maps and institutional affiliations.